Case Studies in Thermal Engineering 47 (2023) 103127

Contents lists available at ScienceDirect

Case Studies in Thermal Engineering

journal homepage: www.elsevier.com/locate/csite

Thrust characteristics research on continuous rotating detonation engine

Qingwu Wang *, Shihui Zhang

Department of Power Engineering, North China Electric Power University, Baoding, 071003, Hebei, China

A R T I C L E I N F O

Handling Editor: Huihe Qiu

Keywords:
Continuous rotating detonation engine
Thrust characteristics
Air-breathing
Pressure enhancement effect

A B S T R A C T

Detonation combustion can produce pressure enhancement effect, increasing engine thrust. In this paper, a 2D Euler control equation with chemical reaction is used to solve the periodic flow of the detonation wave in a rectangular plane. The combustion of the air-breathing continuous rotating detonation engine is simulated. The RDE thrust is obtained through the outlet parameters of the engine. The fuel used is hydrogen, with the equivalent ratio to air. The calculation reflects the working condition of the engine running at low speed. The operating conditions of the engine at low speed are calculated, with a low intake pressure and temperature of 300K and 0.2/0.35 MPa respectively. It is found that the thermal efficiency of detonation wave is higher than that of the deflagration wave under low inlet pressure and temperature, and the thrust of RDE is significantly higher than that of the deflagration engine. The pressure enhancement effect of RDE is not as strong as that of detonation wave, so the pressure ratio of detonation wave can not be used to calculate the engine efficiency.

1. Introduction

Compared with deflagration, detonation has higher thermal efficiency. The RDE has received widespread attention [1,2]. In the air-breathing RDE, the incoming air is compressed by the inlet and mixed with the fuel to, which is burned by the continuous rotating detonation wave (CRDW) propagating in the azimuthal direction. The detonation combustion produces a pressure enhancement effect, and the high-temperature and high-pressure detonation products accelerate to eject to produce thrust. If the air-breathing RDE is combined with the compressor, ground static takeoff can be realized and the engine operating range can be greatly expanded. If it is combined with the turbine, the continuous rotating detonation turbine engine (CRDTE) may be formed.

The thrust performance research of detonation engine includes the analysis model based on detonation wave theory [3,4], the experimental analysis method based on physical model [5,6] and the numerical method based on computational fluid dynamics [7,8]. Each method has its own characteristics and scope of application. The theoretical analysis model is generally based on the ZND model and combined with the engine working cycle to calculate the engine performance parameters.

Some research on the performance simulation and theoretical analysis of the RDE has been carried out. Nordeen, Dunn and others have carried out 1D and 2D analysis of the performance of the RDE [9,10], and confirmed that the thermodynamic efficiency of the RDE is very close to the ideal ZND model; Douglas Schwer et al. simulated the influence of length, diameter, width and other factors of combustion chamber on the propulsion performance, The results showed that the RDE has high performance [11]. Takayuki Yamada et al. simulated the performance of the H 2/O 2 continuous rotary detonation engine with proper chemical equivalence ratio. The

* Corresponding author.
E-mail addresses: wqw@ncepu.edu.cn (Q. Wang), physxzhang@foxmail.com (S. Zhang).

https://doi.org/10.1016/j.csite.2023.103127
Received 16 January 2023; Received in revised form 14 May 2023; Accepted 22 May 2023
Available online 27 May 2023

result show that the fuel specific impulse increases from 2300s to 4000s as the injection pressure increases from 2.0 MPa to 7.0 MPa [12,13]. Lu et al. comprehensively expounded the areas that still need to be further studied in the RDE research and the challenges to be faced in the application of aerospace propulsion [14]. Braun et al. analyzed the air-breathing RDE application range with thermal cycle analysis, and found that the RDE can maintain the aircraft flying at the highest speed Mach 5 [15].

In order to achieve the highest possible thrust performance, the combustion chamber is often designed with high temperature and high pressure, especially for rocket engines. Most of the researches focus on the high inlet total pressure. The researches on the aspirated engine, especially the low inlet pressure, are less.

Different from other studies where the engine inlet pressure exceeds 50 atmospheres, this paper studies the thrust performance of the low-inlet pressure aspirated continuous rotating detonation engine. The thrust of the RDE was compared with that one of the deflagration engine with the same pressure boundary conditions. The difference of engine thrust performance with two combustion conditions of detonation and deflagration was studied.

2. Thrust performance calculation of RDE

In the RDE, the detonation wave moves along the wall of the annular combustion chamber (see Fig. 1) [16]. The thickness of the combustion chamber is relatively small compared with the combustion chamber diameter. The influence of the combustion chamber thickness on the combustion flow field can be ignored. The ring is cut and straightened along the bus bar of the annular combustion chamber, and the cylindrical surface is expanded into a rectangular plane. It is assumed that the rotating detonation wave is a two-dimensional periodic flow in a rectangular plane (see Fig. 2).

The detonation wave moves in the circumferential direction at high speed, and the flow behind the detonation wave has strong circumferential non-uniformity. The whole flow field can be divided into the burned area after the detonation wave and the premixed reactant filling area before the detonation wave. Some of the reactants are combusted by burned by deflagration. Reactant is filled at pressure P_{01} Temperature T_{01}. Due to the detonation wave movement, the filled area has different heights along the circumference. According to C-J theory, air flow after detonation wave is sonic with pressure P_{CJ}. After the wave, the gas flows downstream to expand and accelerate, and becomes supersonic flow. The flow parameters before of the detonation wave are uneven. According to Prandtl-Meyer flow equation, there are slip lines in the flow field. There is an angle between the slip line and the detonation direction. There is also an angle between the oblique shock wave and the detonation direction. The periodic boundary conditions of the rotating detonation flow field lead to the nonuniformity of the flow parameters before the oblique shock wave, which makes the oblique shock wave and the slip line bend.

2.1. Engine thrust performance index parameters

The engine thrust depends on the impulse at the tail nozzle outlet. When the gas at the outlet of engine is in a fully expanded state (that is, when the outlet gas static pressure has the same value as the static pressure ambient), the engine produces the maximum thrust.

The gas impulse at the engine outlet is unevenly distributed along the circumference. The total impulse is:

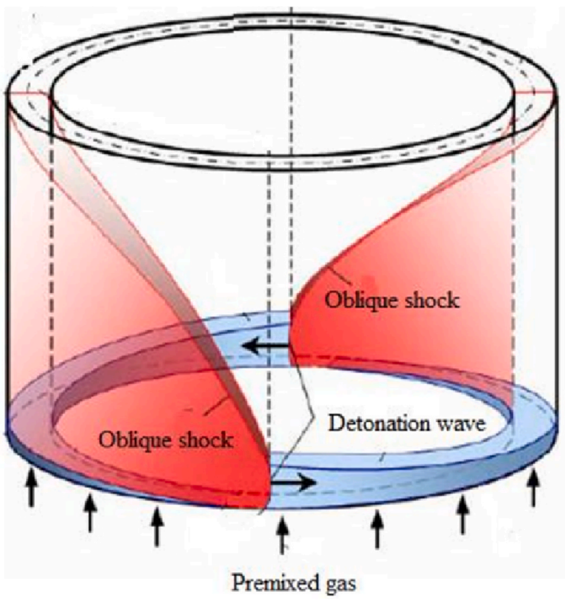

Fig. 1. Annular flow field diagram.

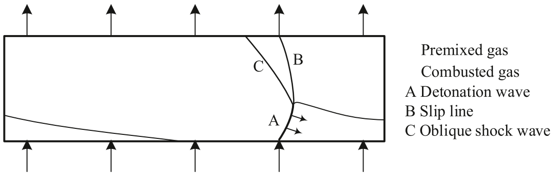

Fig. 2. Plane flow field diagram.

$$I_2 = \int dI_2 = \int Ma_2\sqrt{\gamma RT_2}dm_2$$
$$= \int Ma_2\sqrt{\frac{\gamma RT_{02}}{1+0.5(\gamma-1)Ma_2^2}}dm_2$$
$$= \int \sqrt{\frac{2\gamma}{\gamma-1}}\sqrt{RT_{02}}\sqrt{1-\frac{1}{(P_{02}/P_\infty)^{(\gamma-1)/\gamma}}}dm_2 \quad (1)$$

Where: P_∞ is the ambient static pressure; A_2 is the area at the outlet section; P_2 is the outlet static pressure; P_{02} is the total outlet pressure; T_2 is the outlet static temperature; T_{02} is the total outlet temperature; ρ_2 is the outlet density; Ma_2 is the Mach number of the axial outlet; dm_2 is the outlet mass flow; γ Is the specific heat ratio of gas; R is the gas constant, the gas physical parameters are generally a function of temperature.

The impulse value at outlet is determined by the mass dm_2, total temperature T_{02} and total pressure P_{02}.

Total mass flow is:

$$m_2 = \int dm_2 = \int \rho_2 V_{2y} dx \quad (2)$$

Where: V_{2y} is the axial outlet speed

The engine is required to generate as high thrust as possible with limited fuel. This paper focuses on the combustion impact on engine thrust. It is assumed that there is no loss in the nozzle.

2.2. Verification of numerical method

First, the correctness of the chemical reaction model and numerical method is verified by the one-dimensional detonation wave traveling problem. A 300 mm long detonation tube is used in the calculation. The tube is filled with hydrogen/air mixture of equal equivalence ratio(H_2: O_2: N_2 = 2:1:3.76). The initial gas state in the tube is P = 0.2 MPa, T = 400K. A small section of high temperature and high pressure zone is set at the of tube closed end as the initiation zone: [0,5 mm], P = 3 MPa, T = 6000 K. Uniform grid size Δx = 0.25 is adopted for calculation, with time step Δ T = 10-6 ms. The temperature and pressure calculated at t = 0.12 ms are shown in Fig. 3. In the figure, the pressure and temperature discontinuity are coupled together. The detonation wave characteristics are accurately captured in the calculation. The shock near the initiation zone originates from the strong discontinuity in the high-energy initiation condition, and similar phenomena are also found in many documents. Table 1 shows the calculated overall properties of the detonation wave with the theoretical values [17]. The table includes detonation wave propagation velocity U_D, pressure P_{CJ} and temperature T_{CJ} at Chapman-Jouguet theoretical point. It can be seen that the calculated value is in good agreement with the theoretical value, indicating that the calculation program can accurately simulate the detonation wave.

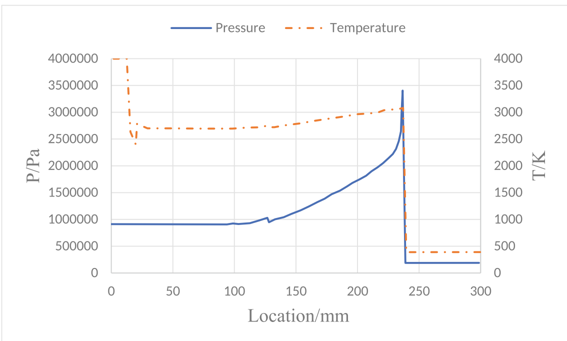

Fig. 3. Temperature and pressure distrubutions of 1D detonation wave.

Tab. 1
Comparison of properies of 1D detontion

methods	U_D/(m/s)	P_{CJ}/MPa	T_{CJ}/K
theoret.	1979.1	2.364	3028.9
comp.	1976.4	2.278	3023.5

2.3. Numerical method

The reaction mixture is 2 H_2 + O_2 +3.76 N_2. N_2 does not participate in the reaction. In this paper, 2D Euler control equation is adopted, based on the ideal gas assumption. The explicit scheme is used to solve the calculation, ignoring the transport effects such as viscosity, heat conduction and diffusion. The three-order MUSCL scheme is used to discretize the convection term, and the four-step Runge-Kutta method with second-order accuracy is used for the time term. The chemical reaction model is a finite rate model, and the reaction rate constant is calculated by Arrhenius formula [18]. The specific heat capacity at constant pressure of each component is a polynomial function of temperature, and the polynomial coefficient is fitted by JANAF Table [19].

The model used for continuous rotating detonation wave calculation is shown in Fig. 4. Because the combustion chamber is annular, the combustion chamber thickness is smaller than the diameter, and the thickness influence on the flow field is ignored. Cut and straighten the ring along the bus bar of the annular combustion chamber to obtain a 2D rectangular area. The calculation area studied in this paper is 20 mm × 100 mm rectangle, with 100 mm circumferential length and 20 mm axial length. It is found that the grid resolution has a certain effect on the calculation results. When the grids number reaches 50000, this effect can be ignored. It can be considered that 50000 grids have met the calculation accuracy requirements, so 50000 grids are selected in this paper.

The upper boundary of the calculation domain is the pressure outlet boundary. There are two cases: when the outlet flow is supersonic, all conserved variables are extrapolated from the internal flow field; When the outlet flow is subsonic, the pressure at the boundary point is equal to the external backpressure and other conserved variables are extrapolated from the internal flow field. The external backpressure is atmospheric pressure, which is taken as 0.1 MPa。

The lower boundary of the computational domain is the inlet boundary. The flow condition of each grid element on the boundary is determined by the grid element pressure P, with three cases.

(1) When $P \geq P_{01}$, the flow is blocked and the injection speed is

$$v = 0 \tag{3}$$

Where, P_{01} is the total injection pressure of the inlet premixed gas. P_{01} Takes 0.2 MPa and 0.35 MPa for calculation

(2) When $P_{01} \geq P \geq P_{cr}$, the injection velocity is calculated according to isentropic expansion:

$$v = \sqrt{\frac{2\gamma}{\gamma - 1} RT_{01} \left[1 - \left(\frac{P}{P_{01}} \right)^{\frac{\gamma-1}{\gamma}} \right]} \tag{4}$$

Where, T_{01} is the total injection temperature, taking 300K; γ is the specific heat ratio of the reaction mixture; R is the gas constant of the reaction mixture; The critical injection pressure is$P_{cr} = P_{01} \left(\frac{2}{\gamma+1} \right)^{\frac{\gamma}{\gamma-1}}$.

(3) When $P < P_{cr}$, the flow is blocked, then:

$$v = \sqrt{\gamma RT_{01} \left(\frac{P_{cr}}{P_{01}} \right)^{\frac{\gamma-1}{\gamma}}} \tag{5}$$

The left and right boundaries of the calculation area are periodic boundaries. The ignition area is a rectangular high temperature 3000K and high pressure 2 MPa area of 9 mm ≤ x ≤ 10 mm, 0 ≤ y ≤ 5 mm.

3. Analysis of calculation results

The calculated temperature distribution is shown in Fig. 5 (a detonation, b deflagration). It can be seen that the temperature in

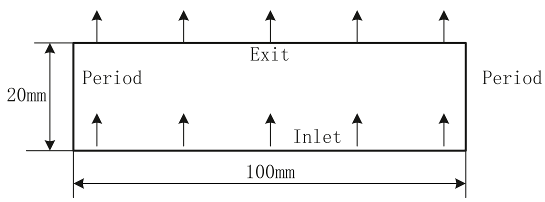

Fig. 4. Schematic diagram of computational domain.

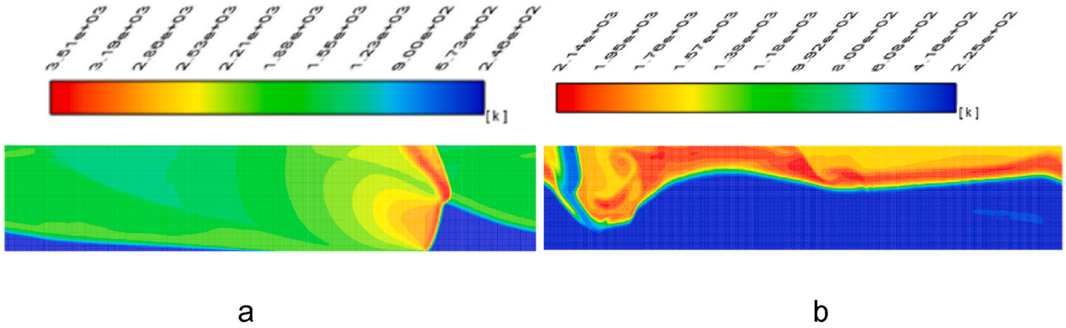

Fig. 5. Temperature contours of computational domain(p01 = 0.2 MPa).

detonation wave is higher than the total temperature at the engine outlet. The total temperature at the outlet of the engine is the maximum temperature that the flame can reach with deflagration. The temperature rise reached by releasing heat is 2100 K, and the temperature in the detonation wave is 3500K. The flame temperature in the detonation wave is 1400K higher than deflagration, as 0.6 times higher.

In addition, the pressure in the detonation wave is higher than the engine outlet. The temperature rise reached by releasing heat is 2100 K and premixed gas temperature is 300 K, which means that the pressure after the detonation wave is about 5 times higher than the engine outlet pressure. But the pressure enhancement effect of detonation wave is not the same as that of engine. The actual total pressure at the engine outlet represents the engine thrust performance. Therefore, the peak pressure measured on the wall cannot be simply used to evaluate the engine performance, otherwise it will lead to misjudgment of the engine thrust performance and get a high thrust value.

The temperature and pressure in the detonation wave are higher than that at the engine outlet. This is because the detonation wave pre-compresses the premixed gas through the shock wave, and then release heat in the compressed gas. This leads to the gas energy contained in the detonation wave, includes work done by pre-compression in addition to combustion heat release. This part of pre-compression work exists to maintain the detonation wave operation and cannot be used to generate thrust, but it is actually reflected in the temperature and pressure in the detonation wave.

The flow field changes periodically. Near the entrance, the transverse detonation wave moves to different positions. At the exit, the oblique shock wave connected with the detonation wave also has different positions. Select the appropriate time point to obtain the same detonation wave location and the inlet total pressure of 0.2 MPa and 0.35 MPa. The outlet total pressure, total temperature and specific impulse obtained from detonation are shown in Figs. 6–8. It can be seen that the detonation engine has the characteristics of self-pressurization, and the outlet total pressure is higher than the inlet total pressure. This is not available for conventional deflagration engines. Deflagration has no pressure enhancement capacity, the outlet total pressure basically has the same value as the inlet, and the pressure enhancement ratio is about 1.

Although the rotating detonation engine has a high pressure enhancement ratio compared with the deflagration engine, the difference between the actual thrust of the two engines is not as large as the combustion pressure enhancement ratio.

The oblique shock wave generated by the detonation wave causes pressure and temperature discontinuity at the outlet plane. Supersonic flow occurs at the outlet plane. When the inlet total pressure is 0.2 MPa, the axial velocity at the outlet plane is significantly lower than that of 0.35 MPa, and the subsonic flow area at the outlet plane becomes larger. With the increase of the inlet total pressure, the detonation wave pressure increases, and the pressure at the outlet plane also increases significantly. Further increasing the total pressure at supersonic speed can not increase the outlet velocity, but can only increase the pressure at the outlet plane. The increase of outlet pressure can also increase the engine specific impulse. With the increase of inlet total pressure, the amplitude of specific impulse increase decreases, which is consistent with the conclusions in many literatures. Since the effect of total pressure on engine thrust is seriously nonlinear, the thrust benefit brought by increasing total pressure will weaken with the increase of total pressure. The

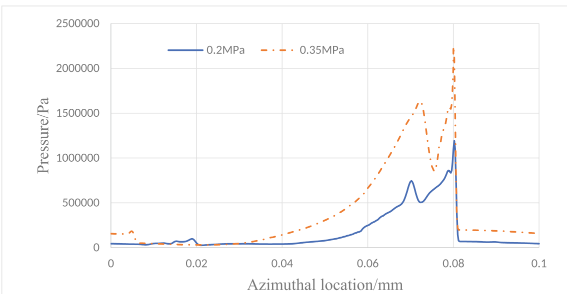

Fig. 6. Pressure distribution at outlet plane.

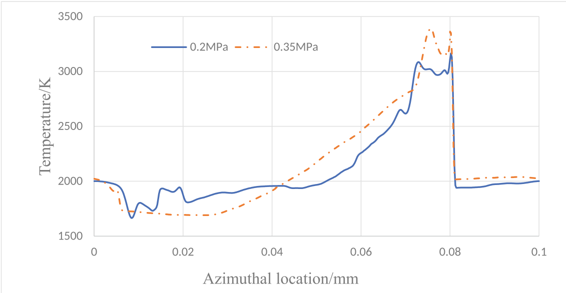

Fig. 7. Temperature distribution at outlet plane.

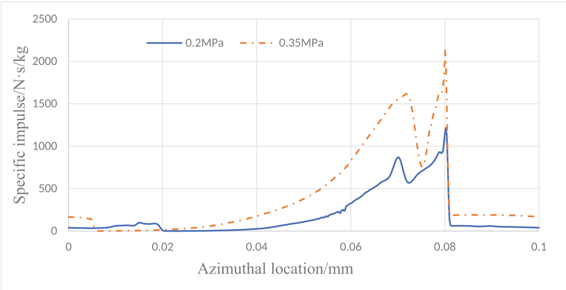

Fig. 8. Specific impulse distribution at outlet plane.

influence curve of total pressure on engine thrust is obtained according to formula (1), as shown in Fig. 9.

Different from deflagration engines, the flow at the outlet of RDE is basically supersonic. Therefore, the Laval Nozzle of detonation engines is not suitable for the RDE. For the RDE, the divergent nozzle may be suitable. In a detonation engine, most of the fuel is burned by detonation, and the rest is burned by deflagration. There is always a certain proportion of deflagration, which is about 24% in this study. This part of deflagration has no contribution to the pressure enhancement effect.

For detonation engines, it can be considered that the flow is uniform. The impulse at the outlet can be set as constant along the circumference, and the total impulse can be written as:

$$I_2 = \sqrt{\frac{2\gamma}{\gamma-1}}\sqrt{RT_{02}}\sqrt{1-\frac{1}{(P_{02}/P_\infty)^{(\gamma-1)/\gamma}}}m_2 \tag{6}$$

Where, m_2 is the mass flow.

Deflagration has no pressure enhancement effect, the outlet total pressure has the same value as the inlet, and the pressure enhancement ratio is about 1. The total pressure at the outlet:

$$P_{02} = P_{01} \tag{7}$$

The total temperature at the outlet:

$$T_{02} = T_{01} + \Delta T \tag{8}$$

Where, ΔT is the heat release temperature rise during combustion。

The specific impulse is calculated as shown in Table 2. The 2D model in this study can also be used to calculate the outlet parameters of the deflagration engine, and the values obtained are consistent with the theoretical calculation values.

In the case of low temperature and pressure, the RDE thrust is higher than deflagration engine, which is the embodiment of the advantages of detonation wave pressure enhancement.

4. Conclusion

In this study, the thrust performance of the air-breathing rotating detonation engine was studied by means of 2D flow simulation. The results show that the detonation wave has self-pressure enhancement characteristics when the temperature and pressure are not too high. The pressure enhancement characteristics of the detonation engine are not as strong as that of the detonation wave. However, the pressure ratio of the detonation wave cannot be used to calculate the efficiency of the engine. This is because the detonation wave pre-compresses the premixed gas through the shock wave, and then release heat in the compressed gas. This part of precompression work exists to maintain the detonation wave operation and cannot be used to generate thrust, but it is actually reflected in the

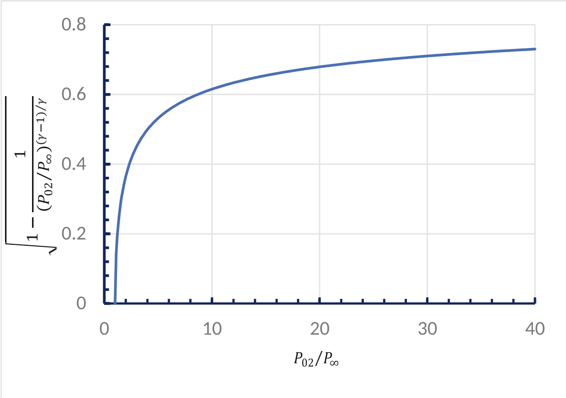

Fig. 9. Pressure effect curve on engine thrust.

Table 2
Thrust characteristics of detonation and deflagration engines.

P_{01} (/MPa)	I_{det}/(N·s/kg)	I_{def}/(N·s/kg)	Increased
0.2	1171.5	715.2	63.8%
0.35	1437.0	934.7	53.7%

temperature and pressure in the detonation wave.

The deflagration engine does not have pressure enhancement characteristics. Similarly, the temperature rise of detonation wave is very high, but the engine is not, which is the same as that of deflagration engine. Although there is about 24% deflagration, the thrust performance is significantly higher than that of deflagration engines. The lower the engine inlet pressure, the more obvious the thrust performance improvement.

Declaration of competing interest

The authors declare that they have no known competing financial interests or personal relationships that could have appeared to influence the work reported in this paper.

Data availability

The data that has been used is confidential.

References

[1] P. Akbari, E. Snyder, Recent Developments in Wave Rotor Combustion Technology and Future Perspectives: a Progress review[R]. AIAA 2007-5055, 2007.
[2] L.S. Langston, Detonation gas turbines, Mechanical engineering (New York, N.Y.: 1919) 135 (12) (2013) 50–54.
[3] E. Wintenberger, J. M. Austin, M. Cooper, S. Jackson, and J. E. Shepherd. An analytical model for the impulse of a single cycle pulse detonation engine [C]. 37th AIAA/ASME/SAE/ASEE Joint Propulsion Conference and Exhibit July 8-11,2001,Salt Lake City, UT. AIAA 2001-3811.
[4] Q. Hua, A. Cx, A. Jl, A theoretical and 1-D numerical investigation on a valve/valveless air-breathing pulse detonation engine - ScienceDirect, Chin. J. Aeronaut. 3 (2020) 500–510.
[5] H.Y. Peng, W.D. Liu, S.J. Liu, et al., Hydrogen-air, ethylene-air, and methane-air continuous rotating detonation in the hollow chamber, Energy 211 (1) (2020), 118598.
[6] G. Wang, W. Liu, S. Liu, et al., Experimental verification of cylindrical air-breathing continuous rotating detonation engine fueled by non-premixed ethylene, Acta Astronaut. 189 (2021) 722–732.
[7] N. Tsuboi, M. Asahara, T. Kojima, et al., Numerical Simulation on Rotating Detonation Engine: Effects of Higher-Order Scheme, 2018.
[8] Z. Rui, W. Jian-Ping, Numerical investigation of flow particle paths and thermodynamic performance of continuously rotating detonation engines, Combust. Flame 159 (12) (2012) 3632–3645.
[9] Nordeen C A, Schwer D, Schauer F, et al. Thermodynamic Modeling of a Rotating Detonation Engine [R].AIAA 2011-803.
[10] I.B. Dunn, V. Malik, W. Flores, et al., Experimental and theoretical analysis of carbon driven detonation waves in a heterogeneously premixed Rotating Detonation Engine, Fuel 302 (2) (2021), 121128.
[11] Schwer D, Kailasanath K. Numerical Study of the Effects of Engine Size on Rotating Detonation Engines [R].AIAA 2011-581.
[12] Yamada T, Hayashi A K, Yamada E, et al. Numerical Analysis of Threshold of Limit Detonation in Rotating Detonation Engine[R]. AIAA 2010-153.
[13] Y. Takayuki, A.K. Hayashi, E. Yamada, et al., Detonation limit thresholds in H 2/O 2 rotating detonation engine, Combust. Sci. Technol. 182 (11–12) (2010) 1901–1914.
[14] F.K. Lu, E.M. Braun, L. Massa, et al., Rotating Detonation Wave Propulsion: Experimental Challenges, Modeling, and Engine Concepts [R]. AIAA-2011-6043, 2011.
[15] Eric M. Braun, Frank Lu, Donald R. Wilson, Airbreathing rotating detonation wave engine cycle analysis, in: 46th AIAA/ASME/SAE/ASEE Joint Propulsion Conference & Exhibit, AIAA 2010-7039, 2010.
[16] D. Kailasanath, Rotating Detonation Engine Research at NRL, 2013.

[17] T.H. Yi, J. Lou, C. Turangan, et al., Propulsive performance of a continuously rotating detonation engine, J. Propul. Power 27 (1) (2011) 171–181.
[18] Shimizu H, Tsuboi N, Hayashi A K Study of Detailed Chemical Reaction Modelon Hydrogen-Air Detonation [R]. AIAA 2001-0478.
[19] D. Stull, H. Prophet, JANAF Thermochemical Tables, 2nd Edition[M], U. S. Government Printing Office, USA, 1971.